Supporting information

Highly Efficient Moisture–Triggered Nanogenerator Based on Graphene Quantum Dots

Yaxin Huang, [†] *Huhu Cheng,*[†,‡] *Gaoquan Shi*[‡] *and Liangti Qu*[†, ǁ, *]

[†] Key Laboratory for Advanced Materials Processing Technology, Ministry of Education of China; State Key Laboratory of Tribology, Department of Mechanical Engineering, Tsinghua University, and [‡] Department of Chemistry, Tsinghua University, Beijing 100084, PR China.

[ǁ] Beijing Key Laboratory of Photoelectronic/Electrophotonic Conversion Materials, School of Chemistry and Chemical Engineering, Beijing Institute of Technology, Beijing 100081, PR China.

* E-mail: lqu@bit.edu.cn

Experimental details

Materials:

Natural graphite powder (325 meshes) was purchased from Qingdao Huatai Lubricant Sealing S&T Co. Ltd (Qingdao, China). Sodium nitrate and sodium carbonate were bought from Xilong Chem. Industry Co., Ltd (Shantou, China). Potassium permanganate and concentrated sulfuric acid were purchased from the Beijing Chemical Reagent Co (Beijing, China).

Preparation of graphene quantum dots with abundant oxygen-containing functional groups:

GQDs was prepared by modified Hummers method according to our previous work. [s1, s2] Typically, 1.0 g graphite was added to 100 mL concentrated sulfuric acid under stirring at room temperature, then 43.0 g sodium nitrate was added and the mixture was cooled to 0 °C. Under vigorous agitation, 3.0 g potassium permanganate was added slowly to make sure the mixture temperature lower than 20 °C. Subsequently, the temperature was heated to 40 °C and stirring for 40 min. The above system was then transferred to a 120 °C oil baths and stirred for 12 h. After that, it was cooled to room temperature and diluted with 500 mL deionized water. The pH of the solution was adjusted with sodium carbonate to about 3. The supernatant was filtered through a 100-nm microporous membrane. Then the solution was centrifuged at 10000 rpm for 1h. The GQDs were collected after the solution was dialyzed in a cellulose ester dialysis bag (cut-off molecular weight 1000 Da) for 3 days.

Fabrication of GQDs based device:

A custom-built metal plate with interdigital gap was used as a mask to fabricate the Au IDE on the flexible Polyethylene terephthalate(PET) matrix by vacuum sputtering methods. The as-prepared IDE on PET substrate with three-finger configuration (the finger width of 250 μm and gap size of 100 μm) exhibited flat surface and sharp edges as observed in optical microscopy, and the corresponding thickness was about 450 nm (Fig. S2). Subsequently, conductive silver adhesives were painted on the IDE fingers to guarantee the schottky contact and facilitate the measurement process. After that, 100 μL GQDs suspensions (ca. 0.1 mg/mL) were added dropwise to the IDE at a slight rotation rate (100 rpm) and natural drying in air for 30 min, thus obtaining the GQDs based device.

Characterization:

The morphology and element of the sample were examined by scanning electron microscope (SEM, JSM-7001F). The morphology of the samples was characterized by using JEM-2010 high resolution transmission electron microscope (HRTEM) at an acceleration voltage of 200 kV. Atomic force microscopic (AFM) images were taken using a Veeco D3100 atomic force microscope. X-ray diffraction (XRD) patterns were obtained by using a Netherlands 1,710 diffractometer with a Cu Kα irradiation source (λ =1.54 Å). Raman spectra were recorded using a RM 2000 Microscopic Confocal Raman Spectrometer (Renishaw PLC, England) with an Ar laser at a wavelength of 514.5 nm. Fourier transform Infra-red (FT-IR) spectra were recorded on a Bruker spectrometer (Equinox 55/S) using KBr pellets. The voltage and current signals were recorded in real time using a Keithley 2612 multimeter, which was controlled by a

LabView-based data acquisition system.

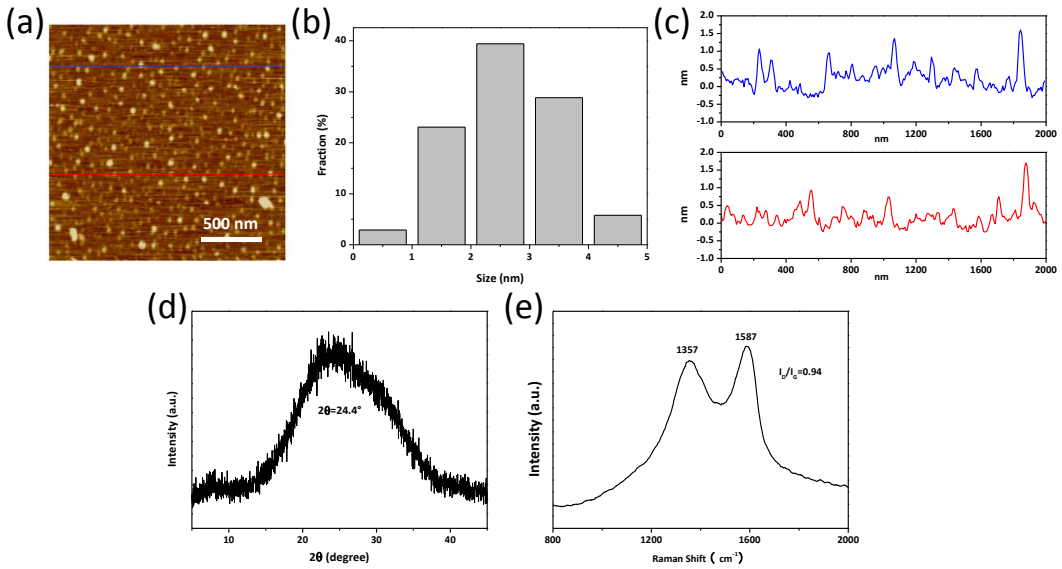

Figure S1. (a) AFM image of GQDs deposited on a mica substrate. (b) Height distribution of GQDs. (c) The height profiles along the lines in (a). (d) XRD pattern of GQDs with a broaden peak centered at 2θ=24.4°, indicating a corresponding d-spacing of 0.36 nm. (e) Raman spectrum of GQDs show apparent disorder D band at 1357 cm^{-1} and graphitic G band at 1587 cm^{-1}. The calculated I_D/I_G ratio is 0.94, suggesting enormous defects existing in as prepared GQDs.

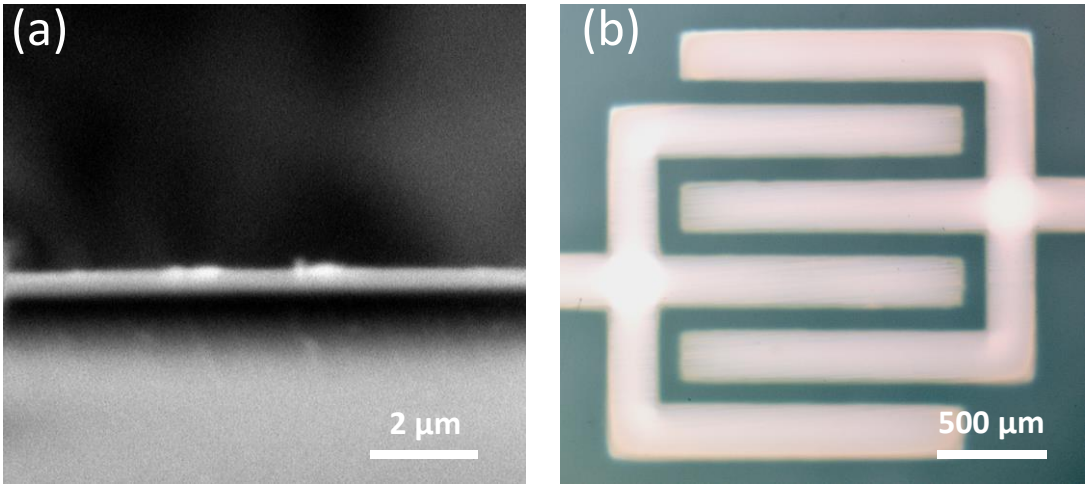

Figure S2. (a) The cross-sectional SEM image of Au IDE. (b) Optical microscopy picture of virgin Au IDE.

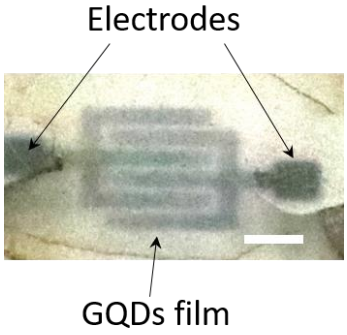

Figure S3. Photograph of GQDs-EG. Scale bar: 500 μm.

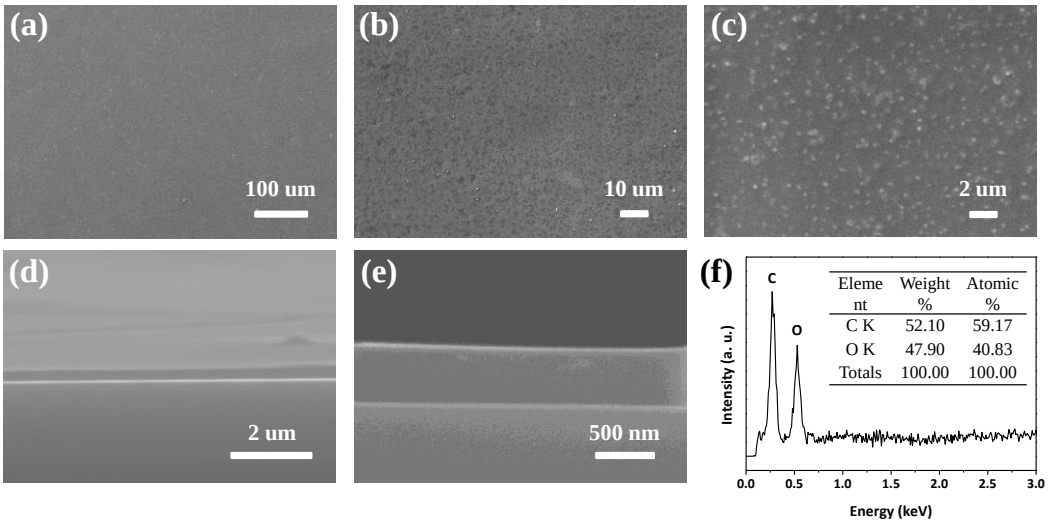

Figure S4. Microstructures and elements of as-synthesized GQDs film. (a-c) SEM images, (d-e) cross-sectional SEM images and (f) EDS spectrum of GQDS film.

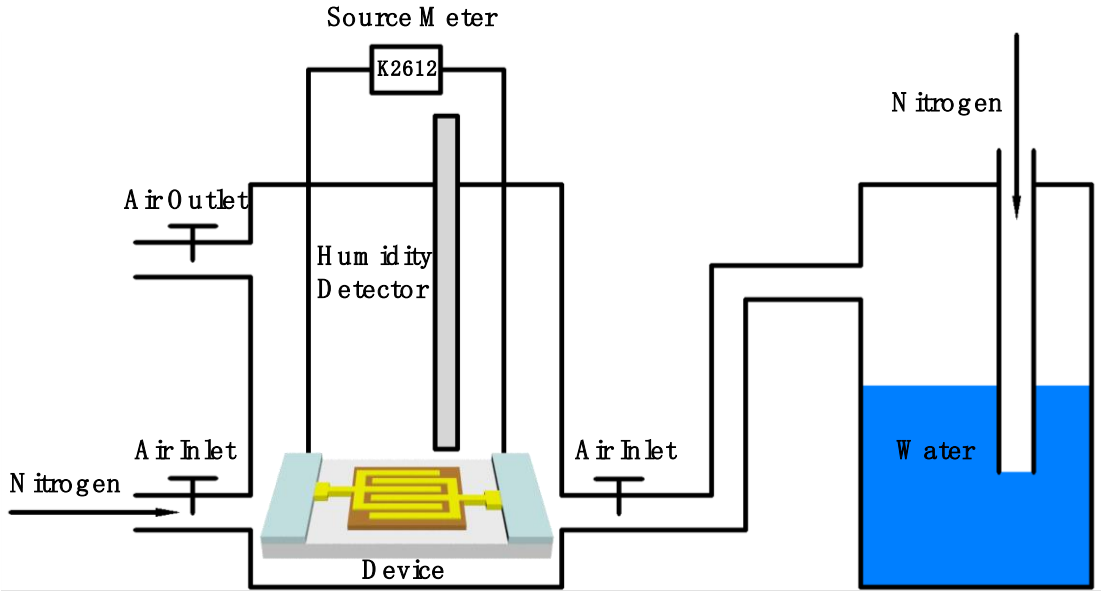

Figure S5. Experimental set-up of the RH controlling system for moisture assisted electrochemical treatment process and MEET process by change the model of source meter. Typically, we simply immobilized the flow rate of the dry nitrogen at a constant speed (1.4 m s^{-1}), tuning the flow rate of the wet nitrogen with different speed to get the variable humidity variation.

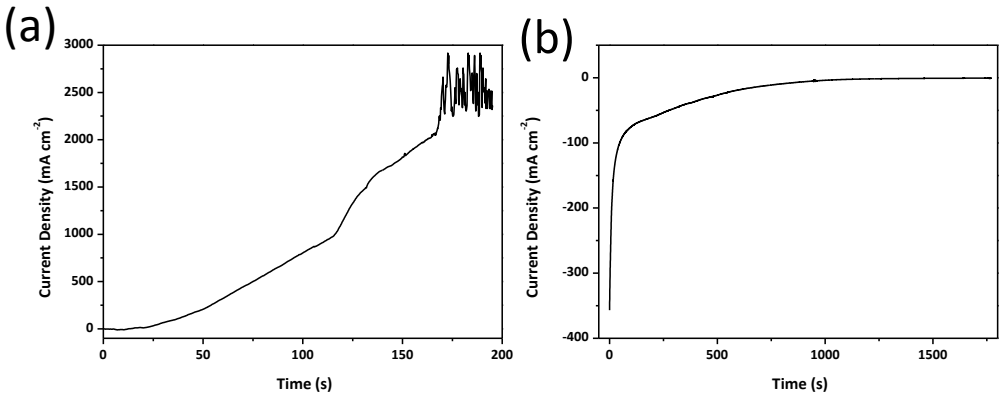

Figure S6. (a) Current-time curves of ECT process under applied voltage of 18 V. (b) Discharge process of GQDs-EG device by short connecting the two electrodes at high

RH atmosphere.

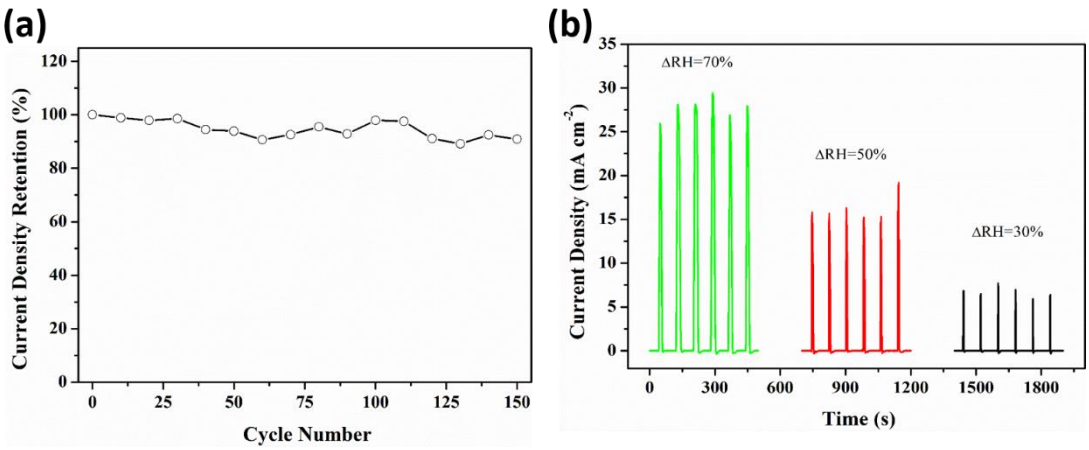

Figure S7. (a)The cycle stability of current output in reply to the change of water content. (b)The dependence of current performance versus the relative humidity variations.

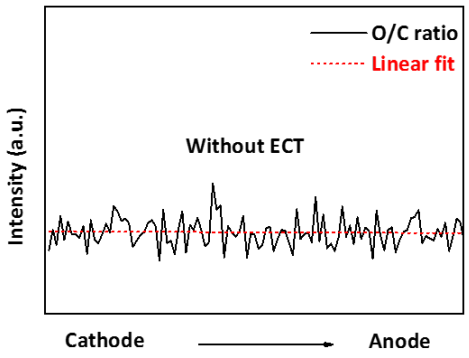

Figure S8. Line scan EDS spectrum of GQDs film without ECT process.

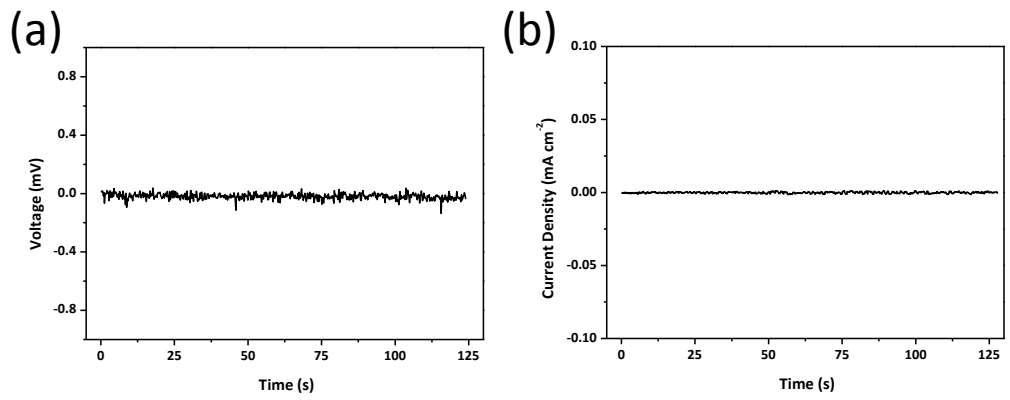

Figure S9. (a) Voltage and (b) current density output of unpolarized GQDs-EG device under moisture tide (△RH=50%).

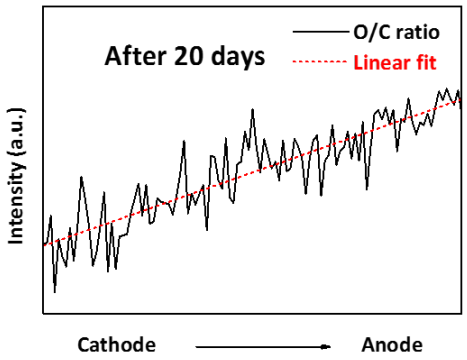

Figure S10. Line scan EDS spectrum of GQDs-EG device after 20 days stored in light resistant condition.

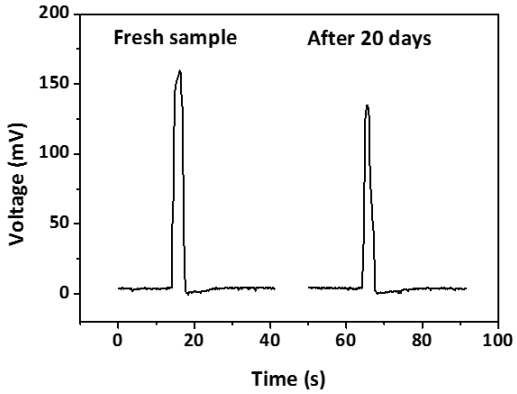

Figure S11. Voltage output of fresh GQDs-EG and GQDs-EG after 20 days stored in light resistant condition.

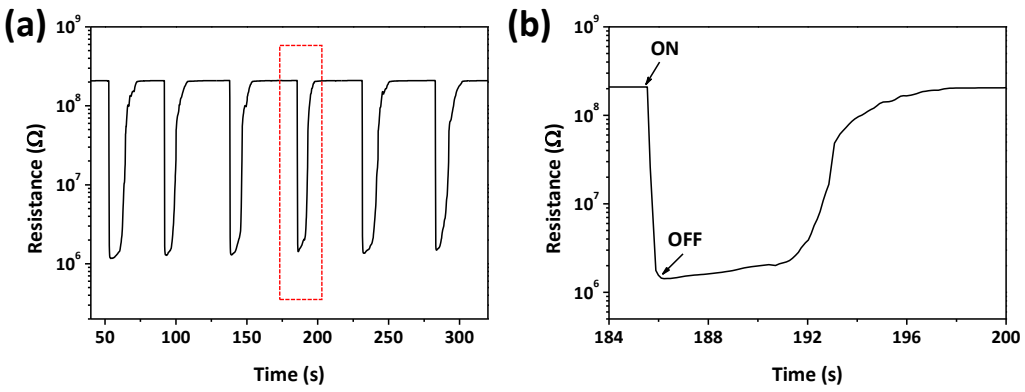

Figure S12. Resistance test cycles (a) and a typical cycle (b) of GQDs-EG upon 50% relative humidity variation.

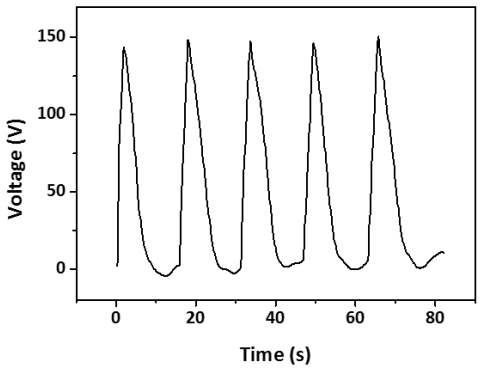

Figure S13. Voltage output cycles of GQDs-EG upon 50% relative humidity variation. The internal time was about 16 s.

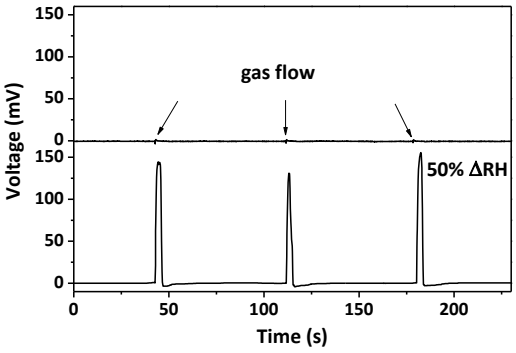

Figure S14. Voltage output of GQDs-EG under gas flow (top) and 50% RH variation (bottom). The flow rate of both was 3.5 m s^{-1}.

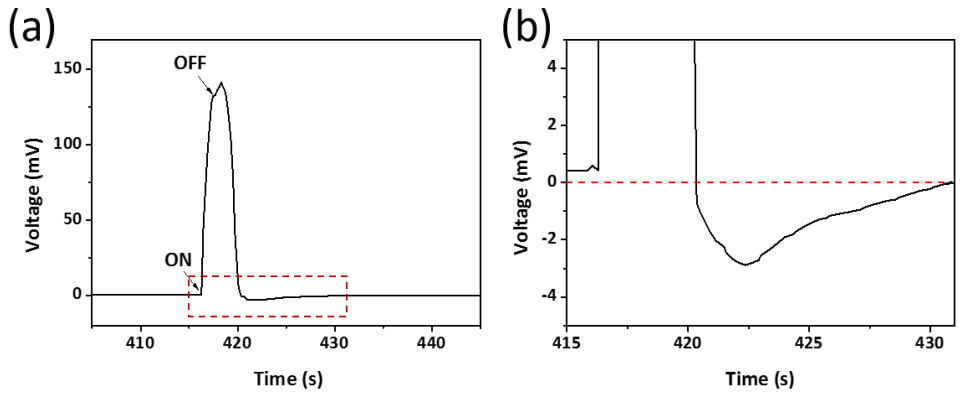

Figure S15. A single voltage output cycle (a) and enlarged-view (b).

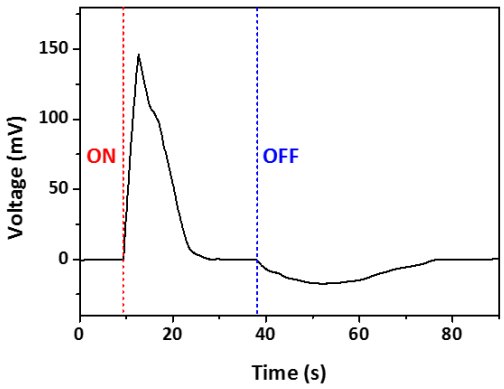

Figure S16. A voltage output cycle exposed upon a constant humidity variation environment. ON and OFF represent the injection and ejection of moisture, respectively.

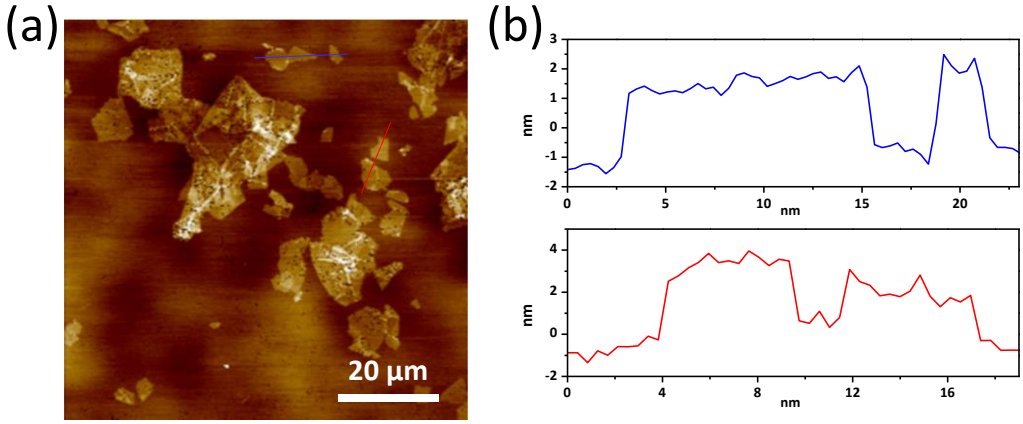

Figure S17. (a) AFM image of GO sheets deposited on a mica substrate. (b) The height profiles of GO sheets.

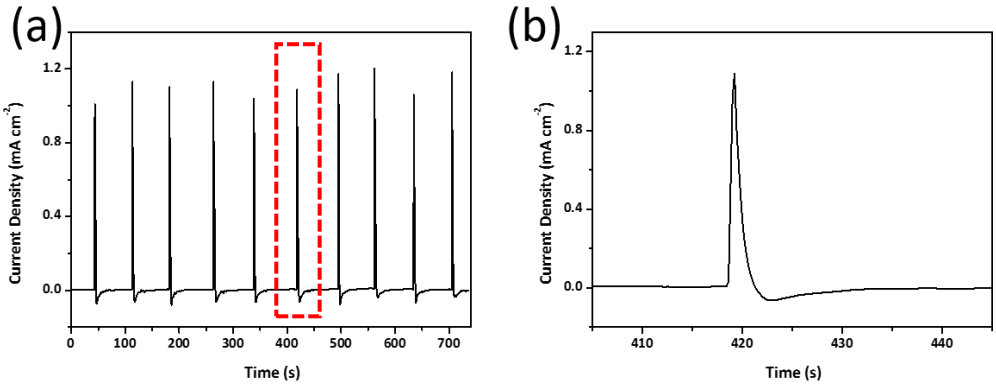

Figure S18. (a) Current output cycles of a typical gradient GO based device in response to the intermittent and periodic relative humidity variation. (b) A typically single cycle current output randomly selected from (a) marked with dashed red lines.

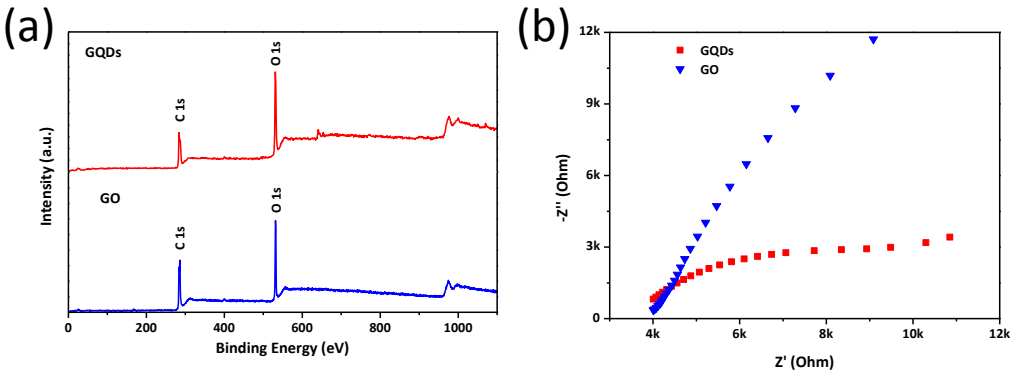

Figure S19. (a) XPS spectrum of GQDs and GO. (b) Electrochemical impedance spectroscopy of GQDs and GO based devices enlarged at high frequency region.

Table S1. Performance of some kinds of water related power generators

	Device Size	Current Density	Voltage	Power Density	Ref.
GO film	0.5 cm×0.5 cm×2.8 μm	9 μA cm^{-2}	30 mV	0.0042 mW cm^{-2}	S3
GO foam	2 cm^2×50 μm	3.2 mA cm^{-2}	260 mV	0.94 mW cm^{-2}	S4
GO nanoribbon	5 mm×5 mm×0.4 mm	0.3 mA cm^{-2}	40 mV	0.012 mW cm^{-2}	S5
GO fiber	1 mm×1 mm×80 μm	1.06 mA cm^{-2}	355 mV	0.376 mW cm^{-2}	S6
Polypyrrole	2 mm×2 mm×100 μm	10 μA cm^{-2}	60 mV	0.0069 mW m^{-2}	S7
Carbon black	1.25 cm×2.5cm×70 μm	105 nA	1250 mV	$4.2*10^{-5}$ mW cm^{-2}	S8
Porous carbon film-1	5 cm×1cm×20 μm	3 nA	68 mV	$3.9*10^{-8}$ mW cm^{-2}	S9
Porous carbon film-2	35 mm×45 mm×15.6 μm	600 nA	900 mV	$3.4*10^{-5}$ mW cm^{-2}	S10
This work	1.5 mm×1.5 mm×0.5 μm	27.7 mA cm^{-2}	270 mV	7.48 mW cm^{-2}	

References

(S1) Wang, L.; Hu, C.; Zhao, Y.; Hu, Y.; Zhao, F.; Chen, N.; Qu, L., A Dually Spontaneous Reduction and Assembly Strategy for Hybrid Capsules of Graphene Quantum Dots with Platinum–copper Nanoparticles for Enhanced Oxygen Reduction Reaction. *Carbon* **2014,** *74*, 170-179.

(S2) Xu, C.; Han, Q.; Zhao, Y.; Wang, L.; Li, Y.; Qu, L., Sulfur-doped Graphitic Carbon Nitride Decorated with Graphene Quantum Dots for an Efficient Metal-free Electrocatalyst. *J. Mater. Chem. A* **2015,** *3* (5), 1841-1846.

(S3) Zhao, F.; Cheng, H.; Zhang, Z.; Jiang, L.; Qu, L., Direct Power Generation from a Graphene Oxide Film under Moisture. *Adv. Mater.* **2015,** *27* (29), 4351-4357.

(S4) Zhao, F.; Wang, L.; Zhao, Y.; Qu, L.; Dai, L., Graphene Oxide Nanoribbon Assembly toward Moisture- powered Information Storage. *Adv. Mater.* **2017,** *29* (3).

(S5) Xue, J.; Zhao, F.; Hu, C.; Zhao, Y.; Luo, H.; Dai, L.; Qu, L., Vapor- activated Power Generation on Conductive Polymer. *Adv. Funct. Mater.* **2016,** *26* (47), 8784-8792.

(S6) Zhao, F.; Liang, Y.; Cheng, H.; Jiang, L.; Qu, L., Highly Efficient Moisture-enabled Electricity Generation from Graphene Oxide Frameworks. *Energy Environ. Sci.* **2016,** *9* (3), 912-916.

(S7) Liu, K.; Yang, P.; Li, S.; Li, J.; Ding, T.; Xue, G.; Chen, Q.; Feng, G.; Zhou, J., Induced Potential in Porous Carbon Films through Water Vapor Absorption. *Angew. Chem.* **2016,** *128* (28), 8135-8139.

(S8) Liang, Y.; Zhao, F.; Cheng, Z.; Zhou, Q.; Shao, H.; Jiang, L.; Qu, L., Self-powered Wearable Graphene Fiber for Information Expression. *Nano Energy* **2017,** *32*, 329-335.

(S9) Xue, G.; Xu, Y.; Ding, T.; Li, J.; Yin, J.; Fei, W.; Cao, Y.; Yu, J.; Yuan, L.; Gong, L., Water-evaporation-induced Electricity with Nanostructured Carbon

Materials. *Nat. Nanotechnol.* **2017,** *12* (4), 317-321.

(S10) Ding, T.; Liu, K.; Li, J.; Xue, G.; Chen, Q.; Huang, L.; Hu, B.; Zhou, J., All-Printed Porous Carbon Film for Electricity Generation from Evaporation-driven Water Flow. *Adv. Funct. Mater.* **2017**, *27* (22), 1700551.